

## Excited state coherent resonant electronic tunneling in quantum well-quantum dot hybrid structures

Yu. I. Mazur, V. G. Dorogan, E. Marega, M. Benamara, Z. Ya. Zhuchenko et al.

Citation: *Appl. Phys. Lett.* **98**, 083118 (2011); doi: 10.1063/1.3560063

View online: <http://dx.doi.org/10.1063/1.3560063>

View Table of Contents: <http://apl.aip.org/resource/1/APPLAB/v98/i8>

Published by the [American Institute of Physics](http://www.aip.org).

### Related Articles

Energy-loss rate of a fast particle in two-dimensional semiconductors with Rashba spin-orbit coupling  
*Appl. Phys. Lett.* **102**, 052113 (2013)

Scattering due to anisotropy of ellipsoid quantum dots in GaAs/InGaAs single quantum well  
*J. Appl. Phys.* **113**, 033701 (2013)

Effect of static carrier screening on the energy relaxation of electrons in polar-semiconductor multiple-quantum-well superlattices  
*J. Appl. Phys.* **113**, 024317 (2013)

Strong coupling at room temperature in ultracompact flexible metallic microcavities  
*Appl. Phys. Lett.* **102**, 011118 (2013)

Configuration interaction in delta-doped heterostructures  
*Low Temp. Phys.* **39**, 28 (2013)

### Additional information on *Appl. Phys. Lett.*

Journal Homepage: <http://apl.aip.org/>

Journal Information: [http://apl.aip.org/about/about\\_the\\_journal](http://apl.aip.org/about/about_the_journal)

Top downloads: [http://apl.aip.org/features/most\\_downloaded](http://apl.aip.org/features/most_downloaded)

Information for Authors: <http://apl.aip.org/authors>

## ADVERTISEMENT

**AIP** | Applied Physics  
Letters

**EXPLORE WHAT'S NEW IN APL**

**SUBMIT YOUR PAPER NOW!**

**SURFACES AND INTERFACES**  
Focusing on physical, chemical, biological, structural, optical, magnetic and electrical properties of surfaces and interfaces, and more...

**ENERGY CONVERSION AND STORAGE**  
Focusing on all aspects of static and dynamic energy conversion, energy storage, photovoltaics, solar fuels, batteries, capacitors, thermoelectrics, and more...

## Excited state coherent resonant electronic tunneling in quantum well-quantum dot hybrid structures

Yu. I. Mazur,<sup>1,a)</sup> V. G. Dorogan,<sup>1</sup> E. Marega, Jr.,<sup>1,b)</sup> M. Benamara,<sup>1</sup> Z. Ya. Zhuchenko,<sup>2</sup> G. G. Tarasov,<sup>2</sup> C. Lienau,<sup>3</sup> and G. J. Salamo<sup>1</sup>

<sup>1</sup>Department of Physics, University of Arkansas, 226 Physics Building, Fayetteville, Arkansas 72701, USA

<sup>2</sup>Institute of Semiconductor Physics, National Academy of Sciences of Ukraine, pr. Nauki 45, Kiev-03028, Ukraine

<sup>3</sup>Institute of Physics, Carl von Ossietzky University, 26129 Oldenburg, Germany

(Received 26 October 2010; accepted 7 February 2011; published online 25 February 2011)

A strong effect of a quantum well (QW) incorporated into a quantum dot (QD) structure on the density of states of the system and the efficiency of carrier transfer from the barrier material to QDs is revealed in InAs/GaAs–InGaAs/GaAs dot-well, tunnel-injection structures. When tuning the QW states in resonance with excited QD states, the carrier flux can be effectively controlled by varying the spacer thickness or barrier height. Enhanced carrier tunneling between QW and QD states is observed by means of photoluminescence excitation spectroscopy for reduced spacer thicknesses. Our results demonstrate that resonant coherent electron tunneling is substantially faster for the second than for the first QW subband and results in the formation of hybrid electronic states delocalized across the QW/QD interface. © 2011 American Institute of Physics.

[doi:10.1063/1.3560063]

Quantum dots (QDs) have been used for various high-performance devices.<sup>1–3</sup> In a QD laser, the carriers initially generated in the barrier material have to be transferred into the QDs before emission can take place. This transfer, due to various scattering mechanisms can reduce the overall device efficiency.<sup>4,5</sup> During relaxation through the discrete states of the QDs carriers interact with a continuum of non-QD states that are weakly coupled to the dots but as a whole have a significant influence on the carrier relaxation.<sup>6–8</sup> Time-resolved photoluminescence (PL) measurements revealed that shortly after a laser pulse excitation this continuum is nearly saturated by short-lived carriers relaxing from the band edge of the barrier material down to the QD ground states.<sup>9</sup> In order to collect and control these carriers, an additional quantum well (QW) can be used similar to that in QW/QD hybrid structures.<sup>10,11</sup>

In this letter, we present the results of spectroscopic studies of InAs/GaAs QDs–In<sub>0.15</sub>Ga<sub>0.85</sub>As/GaAs QW structures in which the QW excitonic state and QD excited state are brought into the resonance. The strength of the resonantly enhanced tunnel coupling is varied by the thickness of the spacer layer that separates the QD and QW structures or by the composition and shape of a complex tunneling barrier. We demonstrate, in particular, that coherent tunneling to neighboring QD states is substantially faster for electrons in the second QW subband than in the first and results in the formation of hybrid electronic states delocalized across the QW/QD interface.

Our samples, grown by molecular beam epitaxy on semi-insulating GaAs (001) substrates after the deposition of ~500 nm GaAs as a buffer, consist of a 14 nm thick In<sub>0.15</sub>Ga<sub>0.85</sub>As QW, a barrier of thickness,  $d_{sp}$ , variable from 1 to 20 nm, and a layer of self-assembled QDs produced by

deposition of a two monolayer thick InAs film. The barriers were grown either as a single continuous GaAs film, or by incorporation of a 1–4 nm thick AlAs layer symmetrically inside the GaAs film. The structures were covered with a 50 nm GaAs cap. For comparison, two reference samples containing solely QD or QW layers were grown under the same growth conditions. Transmission electron microscopy (TEM) analysis proves a high degree of QD (QW) structural similarity between the QD (QW) layers in the different samples of this set. The QD density was  $\sim 10^{10}$  cm<sup>-2</sup> with an average base of  $\sim 20$  nm and height of  $\sim 5$  nm. A representative cross-sectional TEM image is shown in the inset of Fig. 1(a). Low temperature, 10 K, PL measurements were excited with the 532 nm line from a frequency doubled, neodymium doped yttrium aluminum garnet laser with a spot size of  $\sim 20$   $\mu$ m. The PL signal from the sample was dispersed by a monochromator and detected by a liquid nitrogen-cooled InGaAs photodiode array. For the PL excitation (PLE) measurements, a tunable Ti: sapphire laser was used.

Figure 1(a) shows the PL spectra measured in a QW/QD sample with a GaAs spacer thickness of 11 nm for different excitation intensities,  $I_{ex}$ . At low intensity there is a single Gaussian-type band with a maximum at  $\lambda_0^{QD} = 1081$  nm ( $E_0^{QD} = 1.147$  eV with linewidth,  $\Gamma \sim 38$  meV). At the highest  $I_{ex}$ , it transforms into a multiband structure with a dominant feature at  $\lambda_0^{QW} = 923$  nm ( $E_0^{QW} \sim 1.345$  eV, and  $\Gamma \sim 8$  meV) and well-resolvable peaks with maxima at  $\lambda_i^{QD}$  ( $i=0, 1, 2$ ). Comparing these data with the PL spectra of the reference QD and QW samples, we assign  $E_0^{QD}$  and  $E_0^{QW}$  to the QD and QW exciton ground state energies, respectively. The intensity of the QW excitonic emission depends strongly on the barrier thickness. At very low  $I_{ex}$ , only the largest barriers produce a significant QW PL band, as for example in Fig. 1(a). At high  $I_{ex}$ , this band develops along with the emergence of PL from QD excited states at energies,  $E_i^{QD}$ , separated from each other by  $\sim 66$  meV with linewidths of 46–50 meV as determined from a multiple Gaussian fit of the

<sup>a)</sup>Electronic mail: ymazur@uark.edu.

<sup>b)</sup>On leave from Departamento de Física e Ciência dos Materiais, Instituto de Física de São Carlos-USP, São Carlos SP 13560-970, Brazil.

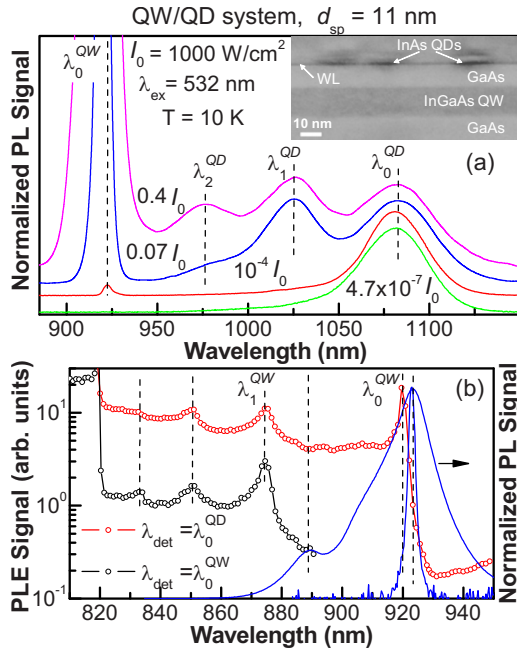


FIG. 1. (Color online) (a) PL spectra for different excitation intensities in a QW/QD hybrid structure with  $d_{sp}=11$  nm. Spectra are vertically shifted for clarity. Inset: cross-sectional TEM image of the structure. (b) PLE spectra measured in dot-well sample at the PL maximum of the QD ground state excitons,  $\lambda_0^{QD}$ , (upper curve), and the PL maximum of the QW ground state exciton,  $\lambda_0^{QW}$ , (lower curve). PL spectra for the reference QW sample are shown at low and high power where an excited state is observed.

spectra. Simulations of the QD energy structure along with the PLE measurements of the reference QD sample established that the QW excitonic ground state at  $E_0^{QW}$  and the third excited QD state  $E_3^{QD}$  are in resonance, which is expected to lead to significantly enhanced coupling between the QDs and QW for a thin spacer. Due to this coupling, the carriers rapidly stream from the QW into the QD states resulting in the observed vanishingly weak intensity of the QW PL at low excitation power. Thus, the resonant coupling transforms the QW into a reservoir that supplies and controls the flux of carriers to the QDs from the GaAs barrier. In order to investigate the energy transfer between the QW and QDs we carried out PLE measurements on a set of samples with varying  $d_{sp}$  and thus varying resonant coupling strength. The PLE spectra provide clear information about the energy transfer between the QW and QDs. Figure 1(b) depicts the PLE spectra detected at  $\lambda_0^{QD}$  and  $\lambda_0^{QW}$  for the same sample as in Fig. 1(a) along with the PL spectra for the reference QW measured at low and high  $I_{ex}$  in order to reveal the QW excited states. Distinct absorption resonances seen in the PLE spectra at  $\lambda=818, 832,$  and  $852$  nm are assigned to the free exciton resonance of the GaAs, and the light and heavy hole excitons in the wetting layer (WL), respectively.<sup>12</sup> These resonances represent the direct absorption and transfer of energy from the GaAs and the WL into the QW and the QDs. In addition, the PLE spectra in Fig. 1(b) show clear excitonic resonances from the first ( $n=0$ ) and second ( $n=1$ ) QW subband at  $\lambda_0^{QW}=923$  nm and  $\lambda_1^{QW}=874$  nm, respectively.<sup>13</sup> Their intensities become strongly dependent on the barrier thickness in hybrid samples, as seen in Fig. 2(a). For a thick barrier ( $d_{sp}=20$  nm) the probability for tunneling between QW and QD states is small and the intensities of the  $\lambda_{0,1}^{QW}$  resonances are weak. With decreasing  $d_{sp}$  the intensity of the QW resonance at  $\lambda_1^{QW}$  increases quickly

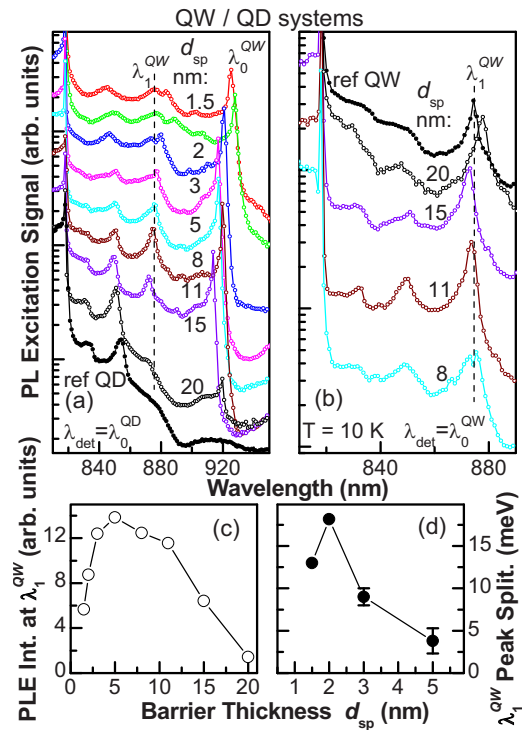


FIG. 2. (Color online) (a) PLE spectra of QW/QD structures with different  $d_{sp}$  values and detection at  $\lambda_0^{QD}$ . The spectra are vertically shifted for clarity. The PLE spectrum of the reference QD sample is at the bottom. (b) QW PLE spectra measured at  $\lambda_0^{QW}$  in the dot-well samples with different  $d_{sp}$  values are given without shift. PLE spectrum of reference QW sample is shown at the top. Summary plot of the PLE peak intensities (c) and splittings (d) at the  $\lambda_1^{QW}$  resonance as a function of the barrier thickness.

reaching a plateau then decreasing again for very thin barriers,  $d_{sp}<5$  nm [Fig. 2(c)]. The spectral shape of the resonance remains nominally the same, showing only a slight broadening and a slight redshift for thin barriers. The redshift may reflect the tunnel-induced mixing of QW and QD wave functions as well as possible strain-induced energy shifts. A similar spectral broadening has been seen before<sup>14</sup> and was explained in terms of a competition between carrier recombination in the QW, QW-QD tunneling, and QD carrier relaxation. The intensity decrease and broadening of the resonance for thin barriers has been taken as a signature for the hybridization of tunnel-coupled QW/QD states. Even more interesting is the pronounced thickness dependence of the second subband resonance at  $\lambda_1^{QW}$ . Here, we find again a strong enhancement in intensity when decreasing the barrier thickness below 15 nm. This saturates then decreases for thinner barriers. For barrier thicknesses between 1.5 and 3 nm a splitting of this resonance into two peaks is observed, energetically separated by 9 meV ( $d_{sp}=3$  nm), 18 meV (2 nm), and 13 meV (1.5 nm), [see Fig. 2(d)]. Such a splitting,  $\omega_R$ , is expected if one assumes resonant coherent tunneling between the QW and QDs resulting in hybridization of the involved electronic states.<sup>15</sup> In the strong coupling limit, this is reached if the tunnel coupling energy,  $\omega_R$ , is larger than the dephasing rates of the excitonic QW and QD excitations, the coupling leads to the formation of hybrid electronic states which are spatially delocalized across the QW/QD interface. The QW/QD coupling can then be understood as a periodic transfer of excitations between QW and QD states with a (Rabi) period of  $t_R=\pi/\omega_R$ . The energy splitting of the PLE resonances is a direct measure of the Rabi period and indi-

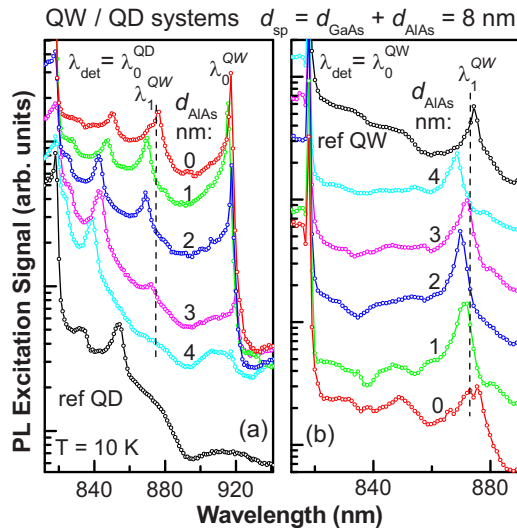


FIG. 3. (Color online) (a) PLE spectra of the QW/QD structures with different thicknesses of the AlAs insertion layer within a constant total barrier thickness  $d_{sp} = d_{GaAs} + d_{AlAs} = 8$  nm. Detection is at  $\lambda_{det} = \lambda_0^{QD}$ . All spectra are given on the same intensity scale and vertically shifted for clarity. (b) QW PLE spectra measured in these samples at  $\lambda_{det} = \lambda_0^{QW}$ .

ates  $t_R = 230$  fs, 115 fs, and 160 fs for  $d_B = 3$  nm, 2 nm, and 1.5 nm, respectively. Such short transfer times are a clear indication that we are observing coherent electron tunneling not hole tunneling, which occurs on a much slower time-scale.<sup>16</sup> We believe that the observation of a coupling-induced splitting for the second QW subband in contrast to only a slight broadening for the lowest QW subband resonances mainly reflects the different electronic wave functions in the  $n=1$  and  $n=2$  QW states. As is well known, the penetration of the ( $n=2$ ) QW electronic wave function into the barrier is much larger than that of the ( $n=1$ ) state. Therefore, the overlap between QW and QD wave functions, and hence the transition rate for tunneling from the QW to the QD (Ref. 16) is enhanced. The ensemble measurements reported here average over a broad inhomogeneous distribution of (localized) QW and QD states which contribute to the tunneling-induced carrier transfer with possibly widely varying Rabi energies. However, our results indicate that—for very thin tunneling barriers—the subpicosecond coherent tunneling dynamics is sufficiently fast to even affect ensemble-averaged spectra. This also implies that nonresonant incoherent tunneling mechanisms, e.g., phonon- or Auger-assisted tunneling are of minor importance.

For narrow spacers, we now have a system with a continuum of states between the energies of the GaAs barrier and QW exciton which can effectively transfer charge carriers from the GaAs barrier to the QD ground state. This allows, e.g., carriers which might be trapped in mid-gap defect states of the barrier or buffer layer to relax to the QD and contribute to the QD emission. The effect of enhancement is strongly controlled by the QW/QD coupling which dramatically changes the density of states function and creates the energy bridges for carrier relaxation.

The tunnel coupling between the QW and QDs is easily demonstrated by changing the effective potential barrier width,  $d_{eff}$ , while holding the geometrical thickness of the spacer constant. This effective barrier is constructed by inserting AlAs layer of different thicknesses symmetrically into the GaAs spacer. The top spectrum in Fig. 3(a) shows that in case of the GaAs spacer of  $d_{sp} = 8$  nm the transfer

efficiency from QW to QD states is high, allowing for a significant enhancement of the carrier transfer from the continuum states into the QDs. Insertion of the AlAs layer in the GaAs spacer increases  $d_{eff}$  and suppresses tunneling from the QW to the QDs. This reduces the transfer efficiency of the structure as is evident by the extinction of the QW absorption lines in the QD PLE for thicker AlAs layers. As can be seen from Fig. 3(b), most of the carriers remain in the QW increasing its efficiency. For  $d_{AlAs} = 4$  nm, QDs and QW layers in the hybrid structure become fully decoupled such that QD and QW emission is similar at low powers.

In summary, the strong effect of incorporating a QW on the density of states and the efficiency of carrier transfer from the barrier material into the QD layer is revealed in InAs/GaAs–InGaAs/GaAs dot-well samples. We demonstrate an enhanced resonant tunnel coupling between QW and QD states by means of PL excitation. Our results show that for the second QW subband the coherent electron tunneling is sufficiently strong to result in the formation of hybrid electronic states which are delocalized across the QW/QD interface with effective transfer times limited by electronic decoherence processes. Hence, the InGaAs QW controls the carrier flux from the GaAs barrier to the InAs QDs, thus defining the effectiveness of tunnel injection structures.

The authors acknowledge the financial support of the MWN (Material World Network) Program between the National Science Foundation of the U.S. (Grant No. DMR-1008107) and the Deutsche Forschungsgemeinschaft (Grant No. Li 580/8-1). C.L. acknowledges also funding from Korea Foundation for International Cooperation of Science & Technology (Global Research Laboratory project, under Grant No. K20815000003).

- <sup>1</sup>H. Shoji, Y. Nakata, K. Mukai, Y. Sugiyama, M. Sugawara, N. Yokoyama, and H. Ishikawa, *Appl. Phys. Lett.* **71**, 193 (1997).
- <sup>2</sup>V. M. Ustinov, A. Y. Egorov, N. A. Maleev, and A. E. Zhukov, *Quantum Dot Lasers* (Oxford University Press, New York, 2003).
- <sup>3</sup>E. U. Rafailov, M. A. Cataluna, and W. Sibbett, *Nat. Photonics* **1**, 395 (2007).
- <sup>4</sup>R. Heitz, H. Born, F. Guffarth, O. Stier, A. Schliwa, A. Hoffmann, and D. Bimberg, *Phys. Rev. B* **64**, 241305(R) (2001).
- <sup>5</sup>J. Urayama, T. B. Norris, J. Singh, and P. Bhattacharya, *Phys. Rev. Lett.* **86**, 4930 (2001).
- <sup>6</sup>Y. Toda, O. Moriawaki, M. Nishioka, and Y. Arakawa, *Phys. Rev. Lett.* **82**, 4114 (1999).
- <sup>7</sup>C. Kammerer, G. Cassabois, C. Voisin, C. Delalande, Ph. Roussignol, and J. M. Gérard, *Phys. Rev. Lett.* **87**, 207401 (2001).
- <sup>8</sup>Yu. I. Mazur, B. L. Liang, Zh. M. Wang, G. G. Tarasov, D. Guzun, and G. J. Salamo, *J. Appl. Phys.* **101**, 014301 (2007).
- <sup>9</sup>Yu. I. Mazur, B. L. Liang, Zh. M. Wang, D. Guzun, G. J. Salamo, G. G. Tarasov, and Z. Ya. Zhuchenko, *J. Appl. Phys.* **100**, 054316 (2006).
- <sup>10</sup>S.-W. Chang, S.-L. Chuang, and N. Holonyak, Jr., *Phys. Rev. B* **70**, 125312 (2004).
- <sup>11</sup>Yu. I. Mazur, B. L. Liang, Zh. M. Wang, D. Guzun, G. J. Salamo, Z. Ya. Zhuchenko, and G. G. Tarasov, *Appl. Phys. Lett.* **89**, 151914 (2006).
- <sup>12</sup>M. Hugues, M. Teisseire, J.-M. Chauveau, B. Vinter, B. Damlano, J.-Y. Duboz, and J. Massies, *Phys. Rev. B* **76**, 075335 (2007).
- <sup>13</sup>R. Heitz, M. Veit, N. N. Ledentsov, A. Hoffmann, D. Bimberg, V. M. Ustinov, P. S. Kop'ev, and Zh. I. Alferov, *Phys. Rev. B* **56**, 10435 (1997).
- <sup>14</sup>Yu. I. Mazur, V. G. Dorogan, D. Guzun, E. Marega, Jr., G. J. Salamo, G. G. Tarasov, A. O. Govorov, P. Vasa, and C. Lienau, *Phys. Rev. B* **82**, 155413 (2010).
- <sup>15</sup>E. A. Stinaff, M. Scheibner, A. S. Bracker, I. V. Ponomarev, V. L. Korenev, M. E. Ware, M. F. Doty, T. L. Reinecke, and D. Gammon, *Science* **311**, 636 (2006).
- <sup>16</sup>S.-L. Chuang and N. Holonyak, Jr., *Appl. Phys. Lett.* **80**, 1270 (2002).